# Measurement of the Generalized Polarizabilities of the Proton in Virtual Compton Scattering at $Q^2$=0.92 and 1.76 GeV$^2$


G. Laveissière,[1] L. Todor,[2] N. Degrande,[3] S. Jaminion,[1] C. Jutier,[1,2] R. Di Salvo,[1] L. Van Hoorebeke,[3] L.C. Alexa,[4] B.D. Anderson,[5] K.A. Aniol,[6] K. Arundell,[7] G. Audit,[8] L. Auerbach,[9] F.T. Baker,[10] M. Baylac,[8] J. Berthot,[1] P.Y. Bertin,[1] W. Bertozzi,[11] L. Bimbot,[12] W.U. Boeglin,[13] E.J. Brash,[4] V. Breton,[1] H. Breuer,[14] E. Burtin,[8] J.R. Calarco,[15] L.S. Cardman,[16] C. Cavata,[8] C.-C. Chang,[14] J.-P. Chen,[16] E. Chudakov,[16] E. Cisbani,[17] D.S. Dale,[18] C.W. de Jager,[16] R. De Leo,[19] A. Deur,[1,16] N. d'Hose,[8] G.E. Dodge,[2] J.J. Domingo,[16] L. Elouadrhiri,[16] M.B. Epstein,[6] L.A. Ewell,[14] J.M. Finn,[7] K.G. Fissum,[11] H. Fonvieille,[1] G. Fournier,[8] B. Frois,[8] S. Frullani,[17] C. Furget,[20] H. Gao,[11,21] J. Gao,[11] F. Garibaldi,[17] A. Gasparian,[22,18] S. Gilad,[11] R. Gilman,[23,16] A. Glamazdin,[24] C. Glashausser,[23] J. Gomez,[16] V. Gorbenko,[24] P. Grenier,[1] P.A.M. Guichon,[8] J.O. Hansen,[16] R. Holmes,[25] M. Holtrop,[15] C. Howell,[21] G.M. Huber,[4] C.E. Hyde-Wright,[2] S. Incerti,[9] M. Iodice,[17] J. Jardillier,[8] M.K. Jones,[7,16] W. Kahl,[25] S. Kato,[26] A.T. Katramatou,[5] J.J. Kelly,[14] S. Kerhoas,[8] A. Ketikyan,[27] M. Khayat,[5] K. Kino,[28] S. Kox,[20] L.H. Kramer,[13] K.S. Kumar,[29] G. Kumbartzki,[23] M. Kuss,[16] A. Leone,[30] J.J. LeRose,[16] M. Liang,[16] R.A. Lindgren,[31] N. Liyanage,[11,31] G.J. Lolos,[4] R.W. Lourie,[32] R. Madey,[5] K. Maeda,[28] S. Malov,[23] D.M. Manley,[5] C. Marchand,[8] D. Marchand,[8] D.J. Margaziotis,[6] P. Markowitz,[13] J. Marroncle,[8] J. Martino,[8] K. McCormick,[2,23] J. McIntyre,[23] S. Mehrabyan,[27] F. Merchez,[20] Z.E. Meziani,[9] R. Michaels,[16] G.W. Miller,[29] J.Y. Mougey,[20] S.K. Nanda,[16] D. Neyret,[8] E.A.J.M. Offermann,[16] Z. Papandreou,[4] B. Pasquini,[33] C.F. Perdrisat,[7] R. Perrino,[30] G.G. Petratos,[5] S. Platchkov,[8] R. Pomatsalyuk,[24] D.L. Prout,[5] V.A. Punjabi,[34] T. Pussieux,[8] G. Quéménér,[7,20] R.D. Ransome,[23] O. Ravel,[1] J.S. Real,[20] F. Renard,[8] Y. Roblin,[1,16] D. Rowntree,[11] G. Rutledge,[7] P.M. Rutt,[23] A. Saha,[16] T. Saito,[28] A.J. Sarty,[35] A. Serdarevic,[4,16] T. Smith,[15] G. Smirnov,[1] K. Soldi,[36] P. Sorokin,[24] P.A. Souder,[25] R. Suleiman,[5,11] J.A. Templon,[10] T. Terasawa,[28] R. Tieulent,[20] E. Tomasi-Gustaffson,[8] H. Tsubota,[28] H. Ueno,[26] P.E. Ulmer,[2] G.M. Urciuoli,[17] M. Vanderhaeghen,[37,7,16] R. Van De Vyver,[3] R.L.J. Van der Meer,[4,16] P. Vernin,[8] B. Vlahovic,[36] H. Voskanyan,[27] E. Voutier,[20] J.W. Watson,[5] L.B. Weinstein,[2] K. Wijesooriya,[7] R. Wilson,[38] B.B. Wojtsekhowski,[16] D.G. Zainea,[4] W-M. Zhang,[5] J. Zhao,[11] and Z.-L. Zhou[11]

(The Jefferson Lab Hall A Collaboration)

[1]*Université Blaise Pascal/IN2P3, F-63177 Aubière, France*
[2]*Old Dominion University, Norfolk, VA 23529*
[3]*University of Gent, B-9000 Gent, Belgium*
[4]*University of Regina, Regina, SK S4S OA2, Canada*
[5]*Kent State University, Kent OH 44242*
[6]*California State University, Los Angeles, CA 90032*
[7]*College of William and Mary, Williamsburg, VA 23187*
[8]*CEA Saclay, F-91191 Gif-sur-Yvette, France*
[9]*Temple University, Philadelphia, PA 19122*
[10]*University of Georgia, Athens, GA 30602*
[11]*Massachusetts Institute of Technology, Cambridge, MA 02139*
[12]*Institut de Physique Nucléaire, F-91406 Orsay, France*
[13]*Florida International University, Miami, FL 33199*
[14]*University of Maryland, College Park, MD 20742*
[15]*University of New Hampshire, Durham, NH 03824*
[16]*Thomas Jefferson National Accelerator Facility, Newport News, VA 23606*
[17]*INFN, Sezione Sanità and Istituto Superiore di Sanità, 00161 Rome, Italy*
[18]*University of Kentucky, Lexington, KY 40506*
[19]*INFN, Sezione di Bari and University of Bari, 70126 Bari, Italy*
[20]*Laboratoire de Physique Subatomique et de Cosmologie, F-38026 Grenoble, France*
[21]*Duke University, Durham, NC 27706*
[22]*Hampton University, Hampton, VA 23668*
[23]*Rutgers, The State University of New Jersey, Piscataway, NJ 08855*
[24]*Kharkov Institute of Physics and Technology, Kharkov 61108, Ukraine*
[25]*Syracuse University, Syracuse, NY 13244*
[26]*Yamagata University, Yamagata 990, Japan*
[27]*Yerevan Physics Institute, Yerevan 375036, Armenia*
[28]*Tohoku University, Sendai 980, Japan*
[29]*Princeton University, Princeton, NJ 08544*
[30]*INFN, Sezione di Lecce, 73100 Lecce, Italy*
[31]*University of Virginia, Charlottesville, VA 22901*
[32]*State University of New York at Stony Brook, Stony Brook, NY 11794*


arXiv:hep-ph/0404243v6 2 Sep 2004

[33]DFNT, University of Pavia and INFN, Sezione di Pavia; ECT*, Villazzano (Trento), Italy
[34]Norfolk State University, Norfolk, VA 23504
[35]Florida State University, Tallahassee, FL 32306
[36]North Carolina Central University, Durham, NC 27707
[37]Institut fuer Kernphysik, University of Mainz, D-55099 Mainz, Germany
[38]Harvard University, Cambridge, MA 02138

We report a Virtual Compton Scattering study of the proton at low CM energies. We have determined the structure functions $P_{LL} - P_{TT}/\epsilon$ and $P_{LT}$, and the electric and magnetic Generalized Polarizabilities (GPs) $\alpha_E(Q^2)$ and $\beta_M(Q^2)$ at momentum transfer $Q^2$= 0.92 and 1.76 GeV$^2$. The electric GP shows a strong fall-off with $Q^2$ and its global behavior does not follow a simple dipole form. The magnetic GP shows a rise and then a fall-off; this can be interpreted as the dominance of a long-distance diamagnetic pion cloud at low $Q^2$, compensated at higher $Q^2$ by a paramagnetic contribution from $\pi N$ intermediate states.

PACS numbers: 13.60.-r,13.60.Fz

The electric and magnetic polarizabilities of the nucleon describe its response to a static electromagnetic field. Contrary to atomic polarizabilities, which are of the size of the atomic volume [1], the proton electric polarizability $\alpha_E$ [2] is much smaller than one cubic fm, the volume scale of a nucleon. Such a small polarizability is a natural indication of the intrinsic relativistic character of the nucleon, as illustrated in a harmonic oscillator model [3]. The smallness of the proton magnetic polarizability $\beta_M$ relative to $\alpha_E$ reflects a strong cancellation of para- and dia-magnetism in the proton.

In Virtual Compton Scattering (VCS) $\gamma^* p \to \gamma p$ the polarizabilities become dependent on the momentum, or the four-momentum transfer $Q^2$ of the virtual photon, as first introduced by Guichon *et al.* [4]. These Generalized Polarizabilities (GPs) can be seen as Fourier transforms of local polarization densities (electric, magnetic, and spin) [5]. Therefore they are a new probe of the nucleon dynamics, allowing e.g. to study the role of the pion cloud and quark core contributions to the nucleon GPs at various length scales. VCS can be accessed experimentally via exclusive photon electroproduction $ep \to ep\gamma$. After the NE-18 experiment [6] and the pioneering VCS experiment at MAMI [7], we performed the E93-050 $\mathrm{H}(e, e'p)\gamma$ experiment [8] at the Thomas Jefferson National Accelerator Facility (JLab). We report low-energy expansion (LEX) analyses of our data up to pion threshold, and Dispersion Relation (DR) analyses of our data extending into the $\Delta$-resonance region.

To lowest order in the fine structure constant $\alpha_{em}$, the unpolarized $ep \to ep\gamma$ cross section at small $q'$ is:

$$\begin{aligned} d^5\sigma^{EXP} &= d^5\sigma^{BH+Born} + q'\phi\Psi_0 + \mathcal{O}(q'^2) , \\ \Psi_0 &= v_1 \cdot (P_{LL} - \frac{1}{\epsilon}P_{TT}) + v_2 \cdot P_{LT} \end{aligned} \tag{1}$$

where $\phi, v_1, v_2$ are kinematical coefficients defined in [9], $q'$ is the final photon energy in the $\gamma p$ CM frame, and $\epsilon$ is the virtual photon polarization. $d^5\sigma^{BH+Born}$ corresponds to the coherent sum of the Bethe-Heitler (BH) and the VCS Born amplitudes, and depends only on the elastic form factors $G_E^p, G_M^p$ of the proton. This is a particular case of Low's low-energy theorem [10] for threshold photon production. The structure functions:

$$\begin{aligned} P_{LL} - \frac{1}{\epsilon}P_{TT} &= \frac{4M_p}{\alpha_{em}} G_E^p(Q^2)\alpha_E(Q^2) + [\text{spin-flip GPs}] \\ P_{LT} &= -\frac{2M_p}{\alpha_{em}}\sqrt{\frac{q^2}{Q^2}} G_E^p(Q^2)\beta_M(Q^2) + [\text{spin-flip GPs}] \end{aligned} \tag{2}$$

contain five of the six independent GPs [11, 12]. These structure functions are defined at fixed $q$, the CM three-momentum of the VCS virtual photon. Equivalently, $Q^2$ in Eqs.(2) is defined in the $q' \to 0$ limit: $Q^2 = 2M_p \cdot (\sqrt{M_p^2 + q^2} - M_p)$.

The apparatus, running conditions and analyses of the JLab experiment are detailed elsewhere [13, 14, 15, 16, 17, 18]. An electron beam of 4.030 GeV energy was directed onto a 15 cm liquid hydrogen target. The two Hall A Spectrometers were used to detect the scattered electron and the outgoing proton in coincidence, allowing the identification of the exclusive reaction $ep \to ep\gamma$ by the missing-mass technique. This experiment makes use of the full capabilities of the accelerator and the Hall A instrumentation [19]: 100% duty cycle, high resolution spectrometers, high luminosities. We summarize our kinematics in Table I. Variables such as $q'$, or the CM polar and azimuthal angles $\theta$ and $\varphi$ of the outgoing photon w.r.t. $\vec{q}$, are obtained by reconstructing the missing particle. The acceptance calculation is provided by a dedicated Monte-Carlo simulation [20] including a model cross section, resolution effects and radiative corrections [21]. A number of cuts are applied in event analysis, especially to obtain a well-defined acceptance and to eliminate protons punching through the spectrometer entrance collimator.

We performed LEX analyses of the data sets I-a and II. The photon electroproduction cross section is determined as a function of $q', \theta$ and $\varphi$ at a fixed value of $q$ (1.080 and 1.625 GeV/c) and $\epsilon$ (0.95 and 0.88, respectively). The effect of the GPs on the cross section is small, reaching at maximum 10-15% below pion threshold. The method to extract the structure functions is deduced from Eq.(1), in which the (BH+Born) cross section is calculated using a recent parametrization of the proton form factors [22].

For each bin in $(\theta, \varphi)$, we measure $d^5\sigma^{EXP}$ in several bins in $q'$, and extrapolate the quantity $\Delta\mathcal{M} = (d^5\sigma^{EXP} - d^5\sigma^{BH+Born})/(\phi q')$ to $q' = 0$, yielding the value of $\Psi_0$. In our data, $\Delta\mathcal{M}$ does not exhibit any significant $q'$-dependence, so the extrapolation to $q' = 0$ is done in each bin in $(\theta, \varphi)$ by averaging $\Delta\mathcal{M}$ over $q'$. The resulting $\Psi_0$ term is then fitted as a linear combination of two free parameters, which are the structure functions $P_{LL} - P_{TT}/\epsilon$ and $P_{LT}$ (Fig. 1).

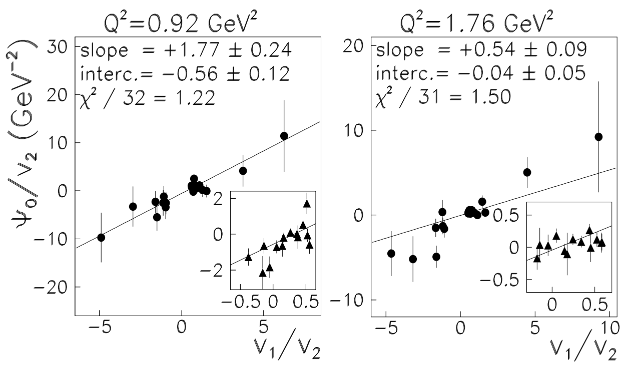


FIG. 1: A graphical representation of the LEX fit (straight line) for data sets I-a and II. Circles correspond to out-of-plane data, and the inner plot is a zoom on the lepton plane data (triangles). $\Psi_0, v_1$ and $v_2$ are defined in the text.

The systematic errors are calculated from four sources added quadratically: 1) $\pm$ 2 MeV uncertainty in beam energy, 2) $\pm$ 0.5 mrad uncertainty in horizontal angles, 3) $\pm$ 2.3% uncertainty in overall absolute cross section normalization, and 4) $\pm$ 2% uncertainty due to possible cross section shape distortions. The value of the reduced $\chi^2$ of the fit (Fig. 1) is one measure of the validity of the LEX in our kinematics. The LEX results for the structure functions are summarized in Table II.

We performed DR analyses of the data sets I-a and II, and also I-b including data from $\pi N$ threshold through the $\Delta$ resonance. In the DR formalism of Pasquini *et al.* [23], the VCS amplitude is determined by unitarity from the MAID $\gamma^{(*)}p \to N\pi$ multipoles [24], plus asymptotic terms $\Delta\alpha$, $\Delta\beta$ which are unconstrained phenomenological contributions to the GPs $\alpha_E(Q^2)$ and $\beta_M(Q^2)$.

TABLE I: Kinematics of $ep \to ep\gamma$. We used data sets I-a and II for the LEX analyses and all data sets for the DR analyses.

| data set | $Q^2$-range (GeV$^2$) | $W$-range |
|---|---|---|
| I-a | [0.85, 1.15] | mostly $< \pi N$ threshold |
| I-b | [0.85, 1.15] | mostly $\Delta(1232)$ resonance |
| II | [1.60, 2.10] | mostly $< \pi N$ threshold |

$\Delta\alpha$, $\Delta\beta$ are parametrized as follows:

$$\Delta\alpha(Q^2) = \alpha_E(Q^2) - \alpha_E^{\pi N}(Q^2) = \frac{[\alpha_E^{exp} - \alpha_E^{\pi N}]_{Q^2=0}}{(1 + Q^2/\Lambda_\alpha^2)^2} \quad (3)$$

(same relation for $\Delta\beta$ with parameter $\Lambda_\beta$) where $\alpha_E^{\pi N}$ ($\beta_M^{\pi N}$) is the $\pi N$ dispersive contribution evaluated from MAID, $\alpha_E^{exp}$ ($\beta_M^{exp}$) is the experimental value at $Q^2 = 0$ [2], and the mass coefficients $\Lambda_\alpha$ and $\Lambda_\beta$ are free parameters. Theoretically, the choice of the dipole form in Eq.(3) is not compulsory. More fundamentally, the DR model provides a rigorous treatment of the higher order terms in the VCS amplitude up to the $N\pi\pi$ threshold, by including resonances in the $\pi N$ channel. In the region of the $\Delta(1232)$ resonance, these higher order terms become dominant over the lowest order GPs given by the LEX.

TABLE II: Compilation of the VCS structure functions. In all cases the first error is statistical, and the second one is the total systematic error.

| | $Q^2$ (GeV$^2$) | $\epsilon$ | $P_{LL} - P_{TT}/\epsilon$ (GeV$^{-2}$) | $P_{LT}$ (GeV$^{-2}$) |
|---|---|---|---|---|
| Ref. | | | Previous experiments | |
| [2] | 0 | | $81.3 \pm 2.0 \pm 3.4$ | $-5.4 \pm 1.3 \pm 1.9$ |
| [7] | 0.33 | 0.62 | $23.7 \pm 2.2 \pm 4.3$ | $-5.0 \pm 0.8 \pm 1.8$ |
| Set | | | This experiment, LEX Analyses | |
| I-a | 0.92 | 0.95 | **1.77** $\pm 0.24 \pm 0.70$ | **-0.56** $\pm 0.12 \pm 0.17$ |
| II | 1.76 | 0.88 | **0.54** $\pm 0.09 \pm 0.20$ | **-0.04** $\pm 0.05 \pm 0.06$ |
| Set | | | This experiment, DR Analyses | |
| I-a | 0.92 | 0.95 | **1.70** $\pm 0.21 \pm 0.89$ | **-0.36** $\pm 0.10 \pm 0.27$ |
| I-b | 0.92 | 0.95 | **1.50** $\pm 0.18 \pm 0.19$ | **-0.71** $\pm 0.07 \pm 0.05$ |
| II | 1.76 | 0.88 | **0.40** $\pm 0.05 \pm 0.16$ | **-0.09** $\pm 0.02 \pm 0.03$ |

The DR analysis consists in fitting the free parameters $\Lambda_\alpha$ and $\Lambda_\beta$ to our cross-section data. This yields the value of the GPs $\alpha_E(Q^2)$ and $\beta_M(Q^2)$ using Eq.(3). This also yields the value of the structure functions of Eqs.(2) since the DR model predicts all the spin-flip GPs [23]. Our DR results are presented in Tables II and III. The systematic uncertainties are calculated from the same sources as in the LEX analyses. The error bars differ from one data set to another, due to differences in phase space coverage and in sensitivity to both the physics and the sources of systematic errors. The reasonably good $\chi^2$ of the DR fits (1.3 to 1.5) indicates that the DR model allows a reliable extraction of GPs in our kinematics, both below and above pion threshold.

Figure 2 shows our DR extraction of the GPs $\alpha_E(Q^2)$ and $\beta_M(Q^2)$, together with the point at $Q^2$= 0 [2] and the points derived from LEX analyses. The latter are obtained by subtracting the spin-flip polarizability predictions [23] to the structure functions of Eqs.(2). This involves some model dependence, which is not presently taken into account in the error bars.

The solid curves in Fig. 2 are the full DR calculations, split into their dispersive $\pi N$ contributions (dashed) and

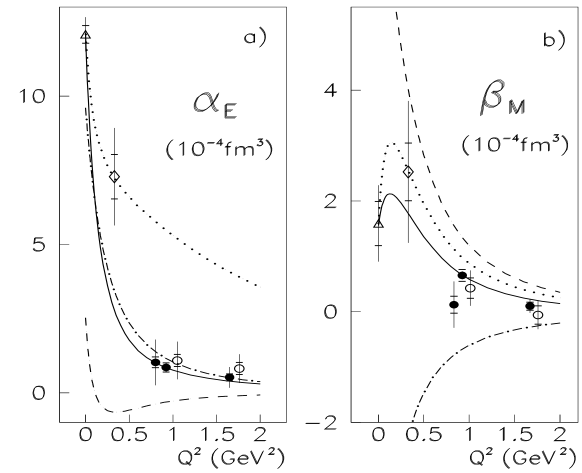


FIG. 2: Compilation of the data on electric (a) and magnetic (b) GPs. Data points are from Ref. [2] (△), the LEX analysis of MAMI [7] (◇), and the present LEX (○) and DR (●) analyses of JLab. Some JLab points are shifted in abscissa for better visibility. The inner error bar is statistical; the outer one is the total error (statistical plus systematic). The curves show calculations in the DR model (see text).

the remaining asymptotic contributions of Eq.(3) (dash-dotted) for $\Lambda_\alpha$=0.70 GeV and $\Lambda_\beta$=0.63 GeV, as fitted to the JLab data set I-b. The $\pi N$ contribution to the magnetic polarizability in Fig. 2-b is strongly paramagnetic, predominantly arising from the $\Delta(1232)$ resonance. In the DR formalism, this is cancelled by a strong diamagnetic term $\Delta\beta$ originating from $\sigma$-meson $t$-channel exchange. The interpretation of $\Delta\beta$ as the contribution of a long-distance pion cloud is further supported by the fact that the fitted scale parameter $\Lambda_\beta$=0.63 GeV is smaller than the elastic form factor dipole parameter $\Lambda$=0.84 GeV. The dotted curves in Fig. 2 result from the full DR calculation, evaluated with $\Lambda_\alpha$=1.79 GeV and $\Lambda_\beta$=0.51 GeV, which reproduces the MAMI LEX data.

TABLE III: The dipole mass parameters $\Lambda_\alpha$ and $\Lambda_\beta$ obtained by fitting the three data sets independently, and the electric and magnetic GPs evaluated at $Q^2$= 0.92 GeV$^2$ (data sets I-a, I-b) and 1.76 GeV$^2$ (data set II). The first and second errors are statistical and total systematic errors, respectively.

| data set | $\Lambda_\alpha$ (GeV) | $\Lambda_\beta$ (GeV) |
|---|---|---|
| I-a | $0.741 \pm 0.040 \pm 0.175$ | $0.788 \pm 0.041 \pm 0.114$ |
| I-b | $0.702 \pm 0.035 \pm 0.037$ | $0.632 \pm 0.036 \pm 0.023$ |
| II | $0.774 \pm 0.050 \pm 0.149$ | $0.698 \pm 0.042 \pm 0.077$ |
| data set | $\alpha_E(Q^2)$ ($10^{-4}$ fm$^3$) | $\beta_M(Q^2)$ ($10^{-4}$ fm$^3$) |
| I-a | $1.02 \pm 0.18 \pm 0.77$ | $0.13 \pm 0.15 \pm 0.42$ |
| I-b | $0.85 \pm 0.15 \pm 0.16$ | $0.66 \pm 0.11 \pm 0.07$ |
| II | $0.52 \pm 0.12 \pm 0.35$ | $0.10 \pm 0.07 \pm 0.12$ |

The data for $\alpha_E(Q^2)$ disagree strongly with the simple dipole ansatz for the contribution $\Delta\alpha$. It should be noted that our DR analysis is basically insensitive to the particular choice of form of $\Delta\alpha$ and $\Delta\beta$, since our fits are performed independently in two small ranges of $Q^2$. Finally we point out that the $\eta N$ and $\pi\pi N$ channels, which must contribute to $\Delta\alpha$, have resonances ($S_{11}(1535)$ and $D_{13}(1520)$, respectively) with transition form factors that do not follow a simple dipole $Q^2$ dependence [25, 26].

In summary, we studied the process $ep \to ep\gamma$ at JLab. With data below pion threshold we applied the LEX, and for data extending through the $\Delta$ resonance we applied the DR formalism to extract the Generalized Polarizabilities. The different analyses are consistent, and the results give new insight into the correlations between spatial and dynamical variables in the proton. Other experiments at low energy will measure the VCS structure functions at low $Q^2$ [27, 28] and separate the six GPs via double polarization measurements [28, 29].

We thank the JLab accelerator staff and the Hall A technical staff for their dedication. This work was supported by DOE contract DE-AC05-84ER40150 under which the Southeastern Universities Research Association (SURA) operates the Thomas Jefferson National Accelerator Facility. We acknowledge additional grants from the US DOE and NSF, the French CNRS and CEA, the Conseil Régional d'Auvergne, the FWO-Flanders (Belgium) and the BOF-Gent University. We thank the INT (Seattle) and ECT* (Trento) for the organization of VCS workshops.

[1] V. A. Dzuba, V. V. Flambaum, and O. P. Sushkov, Phys. Rev. **A56**, R4357 (1997).
[2] V. Olmos de Leon et al., Eur. Phys. J. **A10**, 207 (2001).
[3] B. R. Holstein, D. Drechsel, B. Pasquini, and M. Vanderhaeghen, Phys. Rev. **C61**, 034316 (2000).
[4] P. A. M. Guichon, G. Q. Liu, and A. W. Thomas, Nucl. Phys. **A591**, 606 (1995).
[5] A. I. L'vov, S. Scherer, B. Pasquini, C. Unkmeir, and D. Drechsel, Phys. Rev. **C64**, 015203 (2001).
[6] J. F. J. van den Brand et al., Phys. Rev. **D52**, 4868 (1995).
[7] J. Roche et al., Phys. Rev. Lett. **85**, 708 (2000).
[8] P. Y. Bertin, C. Hyde-Wright, P. A. M. Guichon, et al. (1993), experiment E93-050, URL `http://hallaweb.jlab.org/experiment/E93-050/vcs.html`.
[9] P. A. M. Guichon and M. Vanderhaeghen, Prog. Part. Nucl. Phys. **41**, 125 (1998).
[10] F. E. Low, Phys. Rev. **110**, 974 (1958).
[11] D. Drechsel, G. Knochlein, A. Metz, and S. Scherer, Phys. Rev. **C55**, 424 (1997).
[12] D. Drechsel, G. Knochlein, A. Y. Korchin, A. Metz, and S. Scherer, Phys. Rev. **C57**, 941 (1998).
[13] G. Laveissiere et al., Phys. Rev. **C69**, 045203 (2004).
[14] N. Degrande, Ph.D. thesis, Gent University (2001).
[15] S. Jaminion, Ph.D. thesis, Université Blaise Pascal of Clermont-Fd (2001), DU 1259.
[16] C. Jutier, Ph.D. thesis, Old Dominion University and Université Blaise Pascal of Clermont-Fd (2001), DU 1298.
[17] G. Laveissière, Ph.D. thesis, Université Blaise Pascal of Clermont-Fd (2001), DU 1309.
[18] L. Todor, Ph.D. thesis, Old Dominion University (2000).
[19] J. Alcorn et al., Nucl. Instrum. Meth. Phys. Res. **A522**, 294 (2004).
[20] L. Van Hoorebeke et al., to be submitted to NIM A.
[21] M. Vanderhaeghen et al., Phys. Rev. **C62**, 025501 (2000).
[22] E. J. Brash, A. Kozlov, S. Li, and G. M. Huber, Phys. Rev. **C65**, 051001 (2002).
[23] B. Pasquini, M. Gorchtein, D. Drechsel, A. Metz, and M. Vanderhaeghen, Eur. Phys. J. **A11**, 185 (2001).
[24] D. Drechsel, O. Hanstein, S. S. Kamalov, and L. Tiator, Nucl. Phys. **A645**, 145 (1999).
[25] L. Tiator et al. (2003), nucl-th/0310041.
[26] R. Thompson et al., Phys. Rev. Lett. **86**, 1702 (2001).
[27] J. Shaw, R. Miskimen, et al. (1997), MIT-Bates proposal E97-03.
[28] H. Merkel and N. d'Hose (2000), spokespersons, MAMI Proposal.
[29] M. Vanderhaeghen, Phys. Lett. **B402**, 243 (1997).